Available online at www.sciencedirect.com

ScienceDirect

IFAC PapersOnline CONFERENCE PAPER ARCHIVE

IFAC PapersOnLine 54-14 (2021) 66–71

Undershoot Responses of Circular Path-Following Control for a Vehicle Based on Time-State Control Form

R. Nakata * **M. Tanemura** ** **Y. Chida** ***

* *Graduate School of Science and Technology, Shinshu University, Nagano, Japan, (e-mail: 20w4050e@shinshu-u.ac.jp).*

** *Faculty of Engineering, Shinshu University, Nagano, Japan, (e-mail: tanemura@shinshu-u.ac.jp)*

*** *Faculty of Engineering, Shinshu University, Nagano, Japan, (e-mail: chida@shinshu-u.ac.jp)*

Abstract: In this study, we evaluate a circular path-following control for a vehicle. For a vehicle to follow a circular path, rotational and expansionary coordinate transformations using the time-state control form of the vehicle system is useful. However, an undershoot response occurs in the initial response for some initial conditions. In this study, we derive some conditions with the occurrence of undershoot in the initial response and clarify the conditions for avoiding it. The undershoot analysis of the circular path-following response is performed via numerical simulations using rotational and expansionary coordinate transformations for a vehicle model.

Keywords: Undershoot, Autonomous vehicles, Path-following control, Time-state control form, Nonlinear models

1. INTRODUCTION

In this article, we discuss a circular path-following control for a vehicle. The study on autonomous vehicles is currently underway (Rosas-Vilchis et al. (2020)), particularly for applications in the agricultural field (Iida et al. (2013); Sutisna et al. (2021)). Examples of paths for agricultural vehicles are a straight line and an arbitrary curve, including a circle. Two methods are involved in following a circular path: one is the application of rotational coordinate transformation to the vehicle model (Egami et al. (2005)), and the other is combining the former with expansionary coordinate transformation (Egami et al. (2004)). However, it has been shown that an undershoot in the initial response occurs under specific conditions; the conditions for the undershoot response have also been indicated (Nakata et al. (2020)). Moreover, the latter method suppresses the undershoot response compared with the former. Regarding the undershoot response, a servo control system design without an undershoot response in continuous-time systems (Norimatsu et al. (1961); Mita et al. (1981); Hara et al. (1986)) and the relationship between zeros and the undershoot response in discrete-time systems (Deodhare et al. (1992); De La Barra et al. (1996)) have been discussed. However, the conditions for the undershoot responses differ depending on the transformation of the time-state control form. In this article, we modify the results of previous studies (Nakata et al. (2020, 2021)) and derive conditions for an undershoot response with fewer constraints. Further, we consider the undershoot phenomenon based on the initial conditions of a vehicle.

2. CIRCULAR PATH-FOLLOWING CONTROL WITH ROTATIONAL COORDINATE TRANSFORMATION

2.1 Vehicle model

Herein, we consider the kinematic model of a two-wheeled vehicle shown in Fig. 1. We define P_x, P_y as the center of the vehicle position in the x, y coordinate, ϕ is the angle between the x-axis and the center line of the vehicle, V is the velocity of the center of the vehicle, V_ϕ is the tangential velocity, b is the distance between the center of the vehicle and crawler, and V_l, V_r are the velocities of the left- and right-hand side crawlers, respectively. Then, V, V_ϕ are represented by $V(t) = (V_l(t) + V_r(t))/2, V_\phi(t) = (-V_l(t) + V_r(t))/2b$.

We assume that the vehicle does not slip. The kinematic model whose inputs are V, V_ϕ is as follows (Murray et al. (1993)):

$$\frac{d}{dt}\begin{bmatrix} P_x(t) \\ P_y(t) \\ \phi(t) \end{bmatrix} = \begin{bmatrix} \cos\phi(t) \\ \sin\phi(t) \\ 0 \end{bmatrix} V(t) + \begin{bmatrix} 0 \\ 0 \\ 1 \end{bmatrix} V_\phi(t). \quad (1)$$

We assume that $P_x(t), P_y(t), \phi(t), V(t)$, and $V_\phi(t)$ in Eq. (1) are observable.

2.2 Rotational coordinate transformation

In this section, we discuss the application of rotational coordinate transformation to a vehicle model to follow a circular path. Fig. 2 shows the vehicle model in the d-q plane rotated by θ from the x-y plane. Then, the transformation is expressed as follows (Egami et al. (2005)):

$$\begin{bmatrix} P_d(t) \\ P_q(t) \end{bmatrix} = \begin{bmatrix} \cos\theta(t) & \sin\theta(t) \\ -\sin\theta(t) & \cos\theta(t) \end{bmatrix} \begin{bmatrix} P_x(t) \\ P_y(t) \end{bmatrix}. \quad (2)$$

10.1016/j.ifacol.2021.10.330

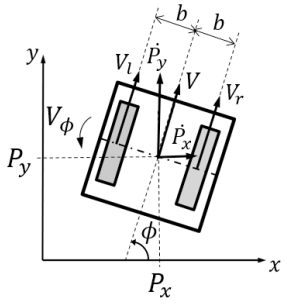

Fig. 1. Vehicle model

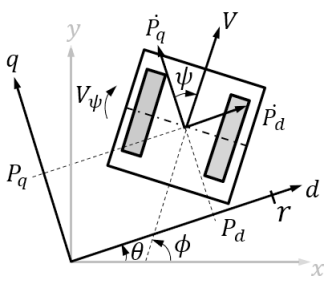

Fig. 2. Vehicle model with the rotational coordinate transformation

Where ψ is the attitude angle in the d, q coordinate, and V_ψ is the tangential velocity of the vehicle. Subsequently, ψ and V_ψ are given by

$$\psi(t) = \frac{\pi}{2} - \phi(t) + \theta(t), \tag{3}$$

$$\dot{\psi}(t) = V_\psi(t). \tag{4}$$

For the circular path-following control, the vehicle is controlled within a circle of radius r =const. by assuming $P_q(t) = \dot{P}_q(t) = 0$. From Eq. (4), the kinematic model of the vehicle is obtained by taking the time derivative of Eq. (2) as follows (Nakata et al. (2020, 2021)):

$$\frac{d}{dt}\begin{bmatrix}\theta(t)\\ P_d(t)\\ \psi(t)\end{bmatrix} = \begin{bmatrix}\cos\psi(t)/P_d(t)\\ \sin\psi(t)\\ 0\end{bmatrix} V(t) + \begin{bmatrix}0\\0\\1\end{bmatrix} V_\psi(t). \tag{5}$$

Equation (5) is a nonholonomic system without a drift term, and it is not stabilized by the static state feedback control (Brockett (1983)). Thus, we discuss the transformation into the time-state control form in the next section.

2.3 Transformation into the time-state control form

This section discusses the time-state control form (Sampei (1994); Sampei et al. (1996)) as a control model. Equation (5) is transformed into Eqs. (8) and (9) of the time-state control form using the coordinate transformation in Eq. (6) and input transformation Eq. (7) as follows (Egami et al. (2005)):

$$\begin{bmatrix}z_1(t)\\ z_2(z_1)\\ z_3(z_1)\end{bmatrix} = \begin{bmatrix}\theta(t)\\ \tan\psi(t)\\ \log|P_d(t)|\end{bmatrix}, \tag{6}$$

$$\begin{bmatrix}V(t)\\ V_\psi(t)\end{bmatrix} = \begin{bmatrix}\mu_v(t)P_d(t)/\cos\psi(t)\\ \mu_v(t)u(z_1)\cos^2\psi(t)\end{bmatrix}, \tag{7}$$

$$\frac{dz_1(t)}{dt} = \mu_v(t), \tag{8}$$

$$\frac{d}{dz_1}\begin{bmatrix}z_3(z_1)\\ z_2(z_1)\end{bmatrix} = \begin{bmatrix}0&1\\0&0\end{bmatrix}\begin{bmatrix}z_3(z_1)\\ z_2(z_1)\end{bmatrix} + \begin{bmatrix}0\\1\end{bmatrix} u(z_1). \tag{9}$$

Equation (8) is the time control part, and Eq. (9) is the state control part. The transformation is valid in the range $|\psi| < \pi/2$, $P_d(t) \neq 0$. $\mu_v(t) > 0$ is set and $z_1(t)$ monotonically increases with time. Therefore, the purpose of Eqs. (8) and (9) is to control $P_d(= e^{z_3} = e^{\log|P_d|})$ to a constant target radius $r(= e^{\log|r|})$ while monotonically increasing $\theta(= z_1)$. In addition, we assume $P_d(t)$ and $\theta(t)$ are observable, and $\psi(t)$ is known through Eq. (3). Thus, z_1, z_2, and z_3 are observable. Further, Eq. (7) is known

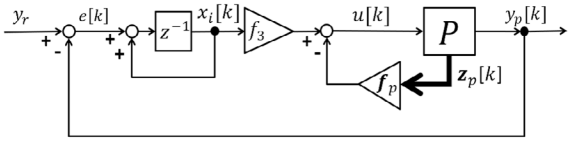

Fig. 3. Servo system with the rotational coordinate transformation

because $\mu_v(t)$ and $u(z_1)$ are obtained from a control law that will be presented later. Hence, $V(t)$ and $V_\psi(t)$ are calculated.

Subsequently, the control model is converted into a discrete-time system. Equation (8) is discretized into Eq. (10) by applying a zero-order hold to the input $\mu_v(t)$ with a sampling period Δt. Equation (9) is discretized into Eq. (11) by applying a zero-order hold to the input $u(z_1)$ with an equivalent sampling period $\Delta z_1(= z_1[k+1] - z_1[k] = \mu_v[k]\Delta t$ =const.) (Nakata et al. (2020, 2021)).

$$z_1[k+1] = z_1[k] + \mu_v[k]\Delta t, \tag{10}$$

$$\boldsymbol{z}_p[k+1] = \boldsymbol{A}_p\boldsymbol{z}_p[k] + \boldsymbol{b}_p u[k], \tag{11}$$

$$\boldsymbol{z}_p[k] := \begin{bmatrix}z_3[k]\\ z_2[k]\end{bmatrix}, \boldsymbol{A}_p := \begin{bmatrix}1&\Delta z_1\\0&1\end{bmatrix}, \boldsymbol{b}_p := \begin{bmatrix}\frac{\Delta z_1^2}{2}\\ \Delta z_1\end{bmatrix}. \tag{12}$$

2.4 Design of servo system

In this article, we design an integral type servo system for a control subject P:

$$P : \begin{cases}\boldsymbol{z}_p[k+1] = \boldsymbol{A}_p\boldsymbol{z}_p[k] + \boldsymbol{b}_p u[k],\\ y_p[k] = \boldsymbol{c}_p\boldsymbol{z}_p[k], \quad \boldsymbol{c}_p = [1\ \ 0],\end{cases} \tag{13}$$

where $y_p = z_3 = \log|P_d|$ is the output (Fig. 3). To facilitate the servo system design, we construct the augmented system as follows:

$$\boldsymbol{z}[k+1] = \boldsymbol{A}\boldsymbol{z}[k] + \boldsymbol{b}u[k] + \boldsymbol{b}_r y_r, \tag{14}$$

$$u[k] = -\boldsymbol{f}\boldsymbol{z}[k], \tag{15}$$

$$\boldsymbol{z}[k] := \begin{bmatrix}\boldsymbol{z}_p[k]\\ x_i[k]\end{bmatrix}, \boldsymbol{A} := \begin{bmatrix}\boldsymbol{A}_p&\boldsymbol{0}\\ -\boldsymbol{c}_p&1\end{bmatrix}, \boldsymbol{b} := \begin{bmatrix}\boldsymbol{b}_p\\0\end{bmatrix}, \boldsymbol{b}_r := \begin{bmatrix}\boldsymbol{0}\\1\end{bmatrix}, \tag{16}$$

$$\boldsymbol{f} := [\boldsymbol{f}_p\ \ -f_3], \boldsymbol{f}_p := [f_1\ \ f_2], \tag{17}$$

where x_i is the state variable of the integrator that accumulates the error between the reference $y_r = \log|r|$ and output y_p. $\boldsymbol{f}$ and $\boldsymbol{f}_p$ are constant feedback gains, and $\boldsymbol{A} - \boldsymbol{b}\boldsymbol{f}$ is a Schur stable matrix. We define Method 1 as the control method of subsection 2.2, subsection 2.3, and subsection 2.4.

2.5 Conditions for avoiding undershoot response

To derive the conditions for avoiding the undershoot response, we determine the conditions for the undershoot response. Here, Type 1 undershoot is defined as the displacement of the output $y_p[k](= z_3[k])$ that is in the opposite direction to the reference value y_r from $k = 0$ to $k = 1$. This situation is represented as follows (De La Barra et al. (1996); Nakata et al. (2020)):

$$(y_r - y_p[0])(y_p[1] - y_p[0]) < 0. \tag{18}$$

From Eq. (18), the condition for avoiding the undershoot response is as follows:

$$(y_r - y_p[0])(y_p[1] - y_p[0]) \geq 0. \tag{19}$$

Equation (19) is rearranged using the control model with rotational coordinate transformation (Eq. (21)). First, from Eqs. (14) and (15), $y_p[1] = z_3[1]$ is given by

$$\begin{aligned} y_p[1] &= z_3[0] + \Delta z_1 z_2[0] \\ &\quad + \frac{1}{2}\Delta z_1^2(-f_1 z_3[0] - f_2 z_2[0] + f_3 x_i[0]), \\ &= y_p[0] + \Delta z_1 z_2[0] - \frac{1}{2}\Delta z_1^2(f_1 y_p[0] + f_2 z_2[0]). \end{aligned} \quad (20)$$

However, we use $x_i[0] = 0$. Notably, $z_2[0] = 0$ was assumed in previous studies (Nakata et al. (2020, 2021)), but we assume that $z_2[0] \neq 0$. Therefore, the conditions for avoiding the undershoot response are obtained by substituting Eq. (20) into Eq. (19) as follows:

$$(y_r - y_p[0])\left(\Delta z_1 z_2[0] - \frac{1}{2}\Delta z_1^2(f_1 y_p[0] + f_2 z_2[0])\right) \geq 0. \quad (21)$$

Here, the following lemma holds.

Lemma 1. For the servo system represented by Eqs. (14) and (15) under the control subject Eq. (11), the necessary and sufficient condition for the feedback gain $\boldsymbol{f} = [f_1, f_2, -f_3]$ that $\boldsymbol{A} - \boldsymbol{b}\boldsymbol{f}$ is a Schur stable matrix satisfies the following inequalities:

$$\begin{aligned} & f_1 > f_3(1 + \frac{a_0}{2a_1}) > 0, \\ & \frac{2}{\Delta z_1} > f_2 > \frac{\Delta z_1(2f_1 - f_3)}{4} > 0, f_3 > 0, \end{aligned} \quad (22)$$

where a_0 and a_1 are defined as

$$\begin{aligned} a_0 &:= 8 - 4\Delta z_1 f_2, \\ a_1 &:= \Delta z_1(-2\Delta z_1 f_1 + 4f_2 + \Delta z_1 f_3). \end{aligned}$$

Proof. See the reference (Nakata et al. (2021)).

From Lemma 1, we obtain the following theorem:

Theorem 1. For the servo system represented by Eqs. (14) and (15), we assume that the feedback gain $\boldsymbol{f}$ is designed such that $\boldsymbol{A} - \boldsymbol{b}\boldsymbol{f}$ is a Schur stable matrix and $x_i[0] = 0$. $y_p[0]$ for avoiding Type 1 undershoot response is as follows:

$$\begin{aligned} & y_p[0] \in H_1 \cup H_2, \\ & H_1 = \{y_p[0] | y_p[0] \leq y_r, y_p[0] \leq \eta\}. \\ & H_2 = \{y_p[0] | y_p[0] \geq y_r, y_p[0] \geq \eta\}. \\ & \eta := \frac{z_2[0]}{f_1}\left(\frac{2}{\Delta z_1} - f_2\right). \end{aligned} \quad (23)$$

Proof. If $y_r - y_p[0] \geq 0$ and

$$\Delta z_1 z_2[0] - \frac{1}{2}\Delta z_1^2(f_1 y_p[0] + f_2 z_2[0]) \geq 0, \quad (24)$$

Eq. (21) is satisfied. From $f_1 > 0$ and $\Delta z_1 > 0$ in Lemma 1, Eq. (24) is equivalent to

$$\begin{aligned} & \frac{2z_2[0]}{\Delta z_1} \geq f_1 y_p[0] + f_2 z_2[0], \\ \Leftrightarrow \quad & y_p[0] \leq \frac{z_2[0]}{f_1}\left(\frac{2}{\Delta z_1} - f_2\right) = \eta. \end{aligned} \quad (25)$$

Therefore, the range of $y_p[0]$ is $y_p[0] \in H_1$.

By contrast, from the conditions that $y_r - y_p[0] \leq 0$ and

$$\Delta z_1 z_2[0] - \frac{1}{2}\Delta z_1^2(f_1 y_p[0] + f_2 z_2[0]) \leq 0, \quad (26)$$

$y_p[0] \in H_2$ is derived similarly.

From the above, $y_p[0]$ for avoiding Type 1 undershoot is represented by $y_p[0] \in H_1 \cup H_2$.

Thus, the following corollary holds.

Corollary 1. For the servo system represented by Eqs. (14) and (15), we assume that the feedback gain $\boldsymbol{f}$ is designed such that $\boldsymbol{A} - \boldsymbol{b}\boldsymbol{f}$ is a Schur stable matrix and $x_i[0] = 0$. The conditions for avoiding Type 1 undershoot are shown using $P_d[0]$ and $\psi[0]$ as follows:

$$\begin{aligned} & P_d[0] \in H_1^* \cup H_2^*, \\ & H_1^* = \{P_d[0] | |P_d[0]| \leq |r|, |P_d[0]| \leq \mathrm{e}^{\eta}\}. \\ & H_2^* = \{P_d[0] | |P_d[0]| \geq |r|, |P_d[0]| \geq \mathrm{e}^{\eta}\}. \\ & \eta := \frac{\tan\psi[0]}{f_1}\left(\frac{2}{\Delta z_1} - f_2\right). \end{aligned} \quad (27)$$

Proof. $P_d[0] \in H_1^* \cup H_2^*$ is derived from substituting $y_p[0] = \log|P_d[0]|$, $z_2[0] = \tan\psi[0]$, and $y_r = \log|r|$ into Eq. (23) in Theorem 1 and the monotonicity of the exponential function as base Napier's number e.

2.6 Control system design and numerical simulation

The control purpose is to make the center of the vehicle follow a circle of radius $r = 0.3$ [m]. The sampling period is $\Delta t = 0.2$ [s], the distance between the center of the vehicle and crawler is $b = 0.15$ [m], and the initial position of the center of the vehicle is $(P_d[0], P_q[0]) = (0.5, 0.0)$ [m]. We designed $\mu_v[k] = V/r = 0.05/0.3$ so that the vehicle on the reference path has a constant-velocity circular motion with a translational velocity of $V = 0.05$ [m/s]. The feedback gains f_1, f_2, and f_3 are designed by the optimal regulator theory based on $\boldsymbol{A}, \boldsymbol{b}$ of Eq. (14) and Eq. (16) with the weight matrices $\boldsymbol{Q}$ and R. To improve the tracking performance of P_d, we set $\boldsymbol{Q}$ =diag$[70, 10, 0.3]$ and $R = 0.2$. The feedback gain is as follows:

$$\boldsymbol{f} = [f_1, f_2, -f_3] = [29.34, 9.564, -1.022].$$

Further, $\boldsymbol{A} - \boldsymbol{b}\boldsymbol{f}$ is Schur stable because the absolute values of the eigenvalues of $\boldsymbol{A} - \boldsymbol{b}\boldsymbol{f}$ are $|0.93 \pm 0.03j| = 0.93$, and 0.81. The initial attitude angle of the vehicle is verified for two cases: $\psi[0] = -45.0$ and 45.0[deg]. In $\psi[0] = -45.0$[deg], $P_d[0] \in H_2^*$ of Eq. (27) is satisfied because $\mathrm{e}^{\eta} = 0.18$. However, Eq. (27) is not satisfied in $\psi[0] = 45.0$[deg] because $\mathrm{e}^{\eta} = 5.6$.

Fig. 4 shows the simulation results. The solid black and red lines represent the reference and response in $\psi[0] = -45.0$[deg], respectively. The dotted blue line represents the response in $\psi[0] = 45.0$[deg]. From Fig. 4, the Type 1 undershoot occurred in $\psi[0] = 45.0$[deg]. By contrast, Type 1 undershoot response did not occur in $\psi[0] = -45.0$[deg]. However, we found another type of undershoot response that moves in the opposite direction after moving to the reference value. This undershoot is referred to as Type 2 undershoot, and is distinguished from the Type 1 undershoot; it is represented by Eq. (18). From the above, when Eq. (23) is satisfied in Method 1, Type 1 undershoot does not occur; however, Type 2 undershoot may occur after the initial response. In the next section, we discuss Type 2 undershoot in detail.

2.7 Verifying Type2 undershoot in Method1

From the simulation results of subsection 2.6, we confirmed that the type of undershoot response depended on the initial conditions of the vehicle. Therefore, we verify the type of undershoot response that is affected by the initial

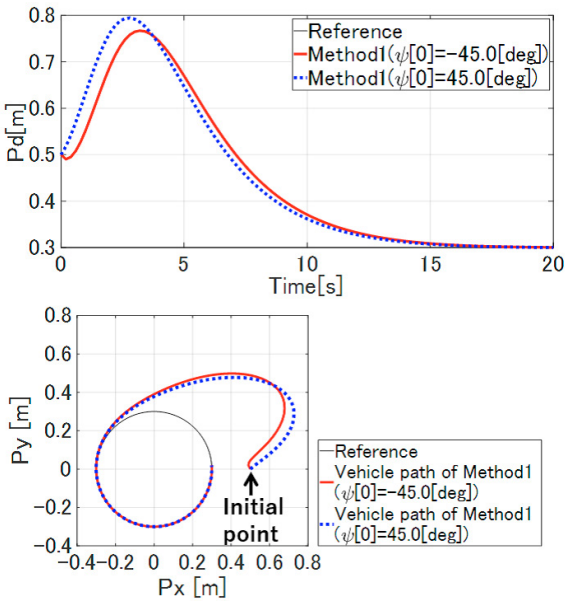

Fig. 4. Simulation results by Method1

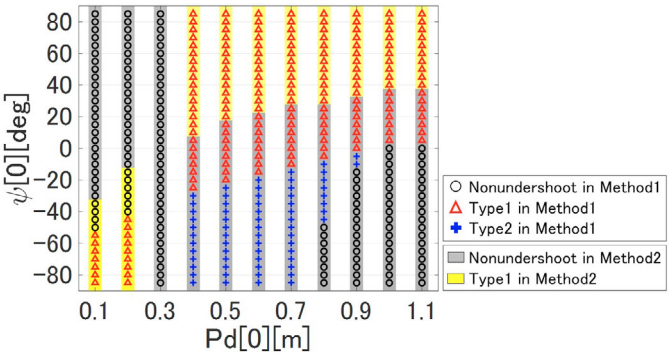

Fig. 5. Initial response analysis by Method1 and Method2

conditions of the vehicle. When Eq. (18) is satisfied, the undershoot response is evaluated as Type 1, whereas, when Eq. (18) is not satisfied and the following equation is satisfied, it is evaluated as Type 2 (Mita et al. (1981)):

$$(y_r - y_p[0])(y_p[k] - y_p[0]) < 0, k \geq 2. \tag{28}$$

The initial values of the vehicle that vary are the attitude angle $\psi[0]$ and initial position $P_d[0]$. The other parameters of the vehicle are similar to those in subsection 2.6. $\psi[0]$ is increased by 5.0[deg] from −85.0[deg] to 85.0[deg], and $P_d[0]$ is increased by 0.1 [m] from 0.1 [m] to 1.1 [m].
Fig. 5 shows the simulation results. The red triangle, blue plus sign, and black circle, respectively, mean that Type 1 undershoot, Type 2 undershoot, and nonundershoot response occurs in the conditions of $P_d[0]$ and $\psi[0]$ in Method 1. The yellow and gray bar show results by Method 2 described in Section 3. From Fig. 5, we confirmed that the existence and types of undershoot phenomena are based on the initial conditions of a vehicle. The undershoot response type in Fig. 4 matched the results of Fig. 5. However, it is a future issue to clarify the relationship between the avoiding and initial conditions of Type 2 undershoot.

3. CIRCULAR PATH-FOLLOWING CONTROL WITH ROTATIONAL AND EXPANSIONARY COORDINATE TRANSFORMATIONS

3.1 Rotational and expansionary coordinate transformations

In this section, we present a method with the expansionary and rotational coordinate transformations presented in Section 2 and define it as Method 2. Let $\hat{P}_d$ and $\hat{P}_q$ be the transformed variables. The vehicle model with the expansionary and rotational coordinate transformations is represented by replacing P_d by $\hat{P}_d$ and P_q by $\hat{P}_q$ in Fig. 2. Using α_d and α_q, which are the expansion coefficients for the d- and q-axis, the expansionary coordinate transformation is expressed as follows (Egami et al. (2004)):

$$\begin{bmatrix} \hat{P}_d(t) \\ \hat{P}_q(t) \end{bmatrix} = \begin{bmatrix} \alpha_d(t) & 0 \\ 0 & \alpha_q(t) \end{bmatrix} \begin{bmatrix} P_d(t) \\ P_q(t) \end{bmatrix}. \tag{29}$$

When the reference is a circular path, we assume that $P_q(t) = \dot{P}_q(t) = \hat{P}_q(t) = \dot{\hat{P}}_q(t) = 0$, and the path error is evaluated on the d-axis similar to Section 2. From the above assumptions, α_q is an arbitrary nonzero constant. When the expansion coefficient for the d-axis is set to $\alpha_d = 1/r$, the reference path is transformed into a unit circle. Taking the time derivative of Eq. (29), the kinematic model of the vehicle is given by (Nakata et al. (2020, 2021)):

$$\frac{d}{dt}\begin{bmatrix} \theta(t) \\ \hat{P}_d(t) \\ \psi(t) \end{bmatrix} = \begin{bmatrix} \alpha_d \cos\psi(t)/\hat{P}_d(t) \\ \alpha_d \sin\psi(t) \\ 0 \end{bmatrix} V(t) + \begin{bmatrix} 0 \\ 0 \\ 1 \end{bmatrix} V_\psi(t). \tag{30}$$

Because Eq. (30) is a nonholonomic system without a drift term, as in Eq. (5), we use the time-state control form presented in the next section.

3.2 Transformation into the time-state control form

The time-state control form with the expansionary and rotational coordinate transformations is represented using the coordinate transformation (Eq. (31)) and the input transformation (Eq. (32)) as follows (Nakata et al. (2020, 2021)):

$$\begin{bmatrix} z_1(t) \\ \hat{z}_2(z_1) \\ \hat{z}_3(z_1) \end{bmatrix} = \begin{bmatrix} \theta(t) \\ \alpha_d \tan\psi(t) \\ \alpha_d \log|\hat{P}_d(t)| \end{bmatrix}, \tag{31}$$

$$\begin{bmatrix} V(t) \\ V_\psi(t) \end{bmatrix} = \begin{bmatrix} \mu_v(t) P_d(t)/\cos\psi(t) \\ \mu_v(t)\hat{u}(z_1)\cos^2\psi(t)/\alpha_d \end{bmatrix}, \tag{32}$$

$$\frac{dz_1(t)}{dt} = \mu_v(t), \tag{33}$$

$$\frac{d}{dz_1}\begin{bmatrix} \hat{z}_3(z_1) \\ \hat{z}_2(z_1) \end{bmatrix} = \begin{bmatrix} 0 & 1 \\ 0 & 0 \end{bmatrix}\begin{bmatrix} \hat{z}_3(z_1) \\ \hat{z}_2(z_1) \end{bmatrix} + \begin{bmatrix} 0 \\ 1 \end{bmatrix}\hat{u}(z_1). \tag{34}$$

Equations (33) and (34) are discretized similarly as in subsection 2.3.

$$z_1[k+1] = z_1[k] + \mu_v[k]\Delta t, \tag{35}$$

$$\hat{\boldsymbol{z}}_p[k+1] = \boldsymbol{A}_p\hat{\boldsymbol{z}}_p[k] + \boldsymbol{b}_p\hat{u}[k], \tag{36}$$

$$\hat{\boldsymbol{z}}_p[k] = [\hat{z}_3[k] \;\; \hat{z}_2[k]]^\mathsf{T},$$

where $\boldsymbol{A}_p$ and $\boldsymbol{b}_p$ are similar to those in Eq. (12).

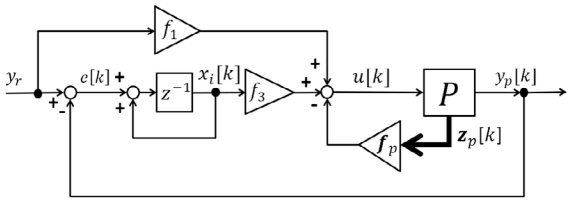

Fig. 6. Servo system with rotational and expansionary coordinate transformations

3.3 Design of servo system

The servo system is designed as in subsection 2.4. The system is obtained by replacing $\boldsymbol{z}_p[k]$ by $\hat{\boldsymbol{z}}_p[k]$, $y_p[k]$ by $\hat{y}_p[k] = \boldsymbol{c}_p\hat{\boldsymbol{z}}_p[k] = \hat{z}_3[k]$, $u[k]$ by $\hat{u}[k]$, $x_i[k]$ by $\hat{x}_i[k] = \alpha_d x_i[k]$, and y_r by $\hat{y}_r = 0(= \log|\alpha_d r| = \log|1|)$ in Fig. 3, Eqs. (14), and (15). From Eq. (14), the augmented system is obtained by substituting the state variable $\boldsymbol{z}[k]$ into $\hat{\boldsymbol{z}}[k] = [\hat{\boldsymbol{z}}_p[k]^\mathsf{T} \ \ \hat{x}_i[k]]^\mathsf{T}$ as follows:

$$\hat{\boldsymbol{z}}[k+1] = \boldsymbol{A}\hat{\boldsymbol{z}}[k] + \boldsymbol{b}\hat{u}[k] + \boldsymbol{b}_r\hat{y}_r = \boldsymbol{A}\hat{\boldsymbol{z}}[k] + \boldsymbol{b}\hat{u}[k], \quad (37)$$

$$\hat{u}[k] = -\boldsymbol{f}\hat{\boldsymbol{z}}[k], \quad (38)$$

where $\boldsymbol{f}$ is the feedback gain defined by Eq.(17) and designed such that $\boldsymbol{A} - \boldsymbol{bf}$ is a Schur stable matrix. Equations (37) and (38) are represented by the following equation in the coordinate system $\boldsymbol{z}[k]$ of Method 1 (Nakata et al. (2020, 2021)):

$$\boldsymbol{z}[k+1] = \boldsymbol{A}\boldsymbol{z}[k] + \boldsymbol{b}u[k] + \boldsymbol{b}_r y_r + \boldsymbol{b}f_1 y_r. \quad (39)$$

The system of Eq. (39) is shown in Fig. 6. The system of Method 2 is equivalent to Fig. 6 and the structure of Method 1 added the feedforward input $f_1 y_r$.

3.4 Conditions for avoiding the undershoot response

In this section, we derive the conditions for avoiding the undershoot response of Method 2; the following theorem holds.

Theorem 2. For the system represented by Eq. (39), we assume that the feedback gain $\boldsymbol{f}$ is designed such that $\boldsymbol{A} - \boldsymbol{bf}$ is a Schur stable matrix and $x_i[0] = 0$. The conditions of $y_p[0]$ for avoiding Type 1 undershoot are as follows:

$$\begin{aligned} &y_p[0] \in H_3 \cup H_4, \quad (40)\\ &H_3 = \{y_p[0] | y_p[0] \le y_r, y_p[0] \le \eta + y_r\}.\\ &H_4 = \{y_p[0] | y_p[0] \ge y_r, y_p[0] \ge \eta + y_r\}. \end{aligned}$$

Proof. We assume that $x_i[0] = 0$. From Eq. (39), $y_p[1]$ is expressed as follows:

$$y_p[1] = z_3[0] + \Delta z_1 z_2[0] - \frac{1}{2}\Delta z_1^2(f_1 z_3[0] + f_2 z_2[0] - f_1 y_r). \quad (41)$$

The condition of $y_p[0]$ for avoiding Type 1 undershoot is obtained by substituting Eq. (41) into Eq. (19) as follows:

$$(y_r - y_p[0])\left(\Delta z_1 z_2[0] - \frac{1}{2}\Delta z_1^2(f_1 y_p[0] + f_2 z_2[0] - f_1 y_r)\right) \ge 0. \quad (42)$$

The condition of Eq. (42) is divided into two cases whether $y_r - y_p[0] \ge 0$ or $y_r - y_p[0] \le 0$ by the similar manner described in the proof of Theorem 1. If $y_r - y_p[0] \ge 0$ and

$$\Delta z_1 z_2[0] - \frac{1}{2}\Delta z_1^2(f_1 y_p[0] + f_2 z_2[0] - f_1 y_r) \ge 0, \quad (43)$$

Eq. (42) is satisfied. From $f_1 > 0$ and $\Delta z_1 > 0$ of Lemma 1, Eq. (43) becomes equivalent to

$$\begin{aligned} &\frac{2z_2[0]}{\Delta z_1} \ge f_1 y_p[0] + f_2 z_2[0] - f_1 y_r\\ \Leftrightarrow \quad &y_p[0] \le \eta + y_r \end{aligned} \quad (44)$$

Therefore, the range of $y_p[0]$ is as follows $y_p[0] \in H_3$.
By contrast, from the conditions that $y_r - y_p[0] \le 0$ and

$$\Delta z_1 z_2[0] - \frac{1}{2}\Delta z_1^2(f_1 y_p[0] + f_2 z_2[0] - f_1 y_r) \le 0, \quad (45)$$

$y_p[0] \in H_4$ is derived.
Consequently, $y_p[0]$ for avoiding Type 1 undershoot is represented by $y_p[0] \in H_3 \cup H_4$.

From Theorem 2, the following corollary holds.

Corollary 2. For the system represented by Eq. (39), we assume that the feedback gain $\boldsymbol{f}$ is designed such that $\boldsymbol{A} - \boldsymbol{bf}$ is a Schur stable matrix and $x_i[0] = 0$. Then, using $P_d[0]$ and $\psi[0]$, the conditions for avoiding Type 1 undershoot are as follows:

$$\begin{aligned} &P_d[0] \in H_3^* \cup H_4^*, \quad (46)\\ &H_3^* = \{P_d[0] | |P_d[0]| \le |r|, |P_d[0]| \le \mathrm{e}^\eta |r|\}.\\ &H_4^* = \{P_d[0] | |P_d[0]| \ge |r|, |P_d[0]| \ge \mathrm{e}^\eta |r|\}.\\ &\eta := \frac{\tan\psi[0]}{f_1}\left(\frac{2}{\Delta z_1} - f_2\right). \end{aligned}$$

We consider the conditions of Eq. (46). In $|P_d[0]| \le |r|$, when $|P_d[0]| \le \mathrm{e}^\eta |r|$ is satisfied, Type 1 undershoot does not occur. The sign of η matched the sign of $\psi[0]$ because $f_1 > 0$ and $2/\Delta z_1 > f_2$ in Lemma 1. Therefore, when $\psi[0] \ge 0$ holds, $P_d[0] \in H_3^*$ is satisfied because $\mathrm{e}^\eta \ge 1$, which implies that the vehicle tilts toward the reference path in the initial conditions. H_4^* is derived in similarly to the above idea. Therefore, in Method 2, Type 1 undershoot is avoided if the initial attitude angle of the vehicle is set in the same direction to the reference path exist. Further, Type 1 undershoot is prevented if H_3^* and H_4^* make larger set. Therefore, it is effective by increasing f_1 and f_2 because η is smaller in (46).

3.5 Numerical simulation

We execute a numerical simulation under the same conditions as in subsection 2.6. In the initial condition $\psi[0] = -45.0$[deg], $P_d[0] \in H_4^*$ is satisfied because $\mathrm{e}^\eta = 0.18$. However, in $\psi[0] = 45.0$[deg], the initial conditions of the vehicle do not satisfy Eq. (46) because $\mathrm{e}^\eta = 1.7$.
Fig. 7 shows the simulation results. The solid black and red lines represent the reference and response in $\psi[0] = -45.0$[deg], respectively. The dotted blue line represents the response in $\psi[0] = 45.0$[deg]. From Fig. 7, undershoot responses were avoided in $\psi[0] = -45.0$[deg], and the Type 1 undershoot occurred in $\psi[0] = 45.0$[deg].

3.6 Comparison of the initial conditions for the occurrence of the undershoot response in Method1 *and* Method2

Similar to subsection 2.7, we evaluate the undershoot response by numerical simulation. Fig. 5 shows the simulation results. The yellow and gray bars mean that Type 1 undershoot and nonundershoot occur in the conditions of $P_d[0]$ and $\psi[0]$ in Method 2. We compare the methods in terms of the initial conditions for the occurrence of

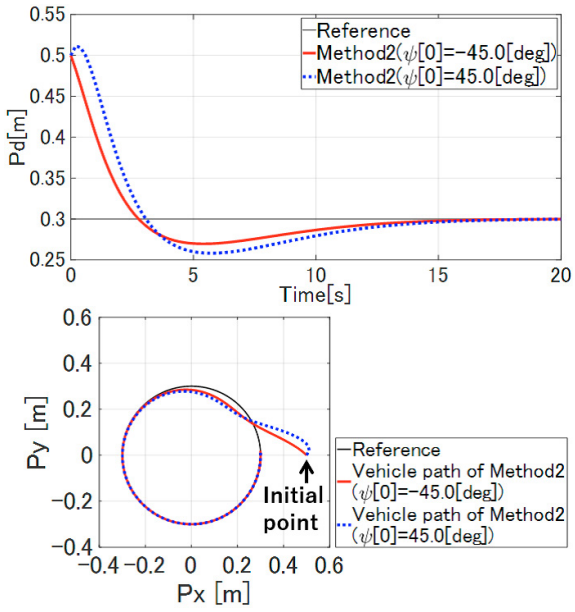

Fig. 7. Simulation results by Method2

the undershoot response. The number of conditions under which Type 1 undershoot occurred using Methods 1 and 2 is 173 and 124, respectively. Hence, we confirm that Method 2 avoided Type 1 undershoot more than Method 1 within the range of the initial conditions of the vehicle set in this simulation. Moreover, from Fig. 5, Type 2 undershoot does not occur under these conditions using Method 2. As a result, the feedforward input is effective to suppress Type 2 undershoot. It is a future study to derive a condition for avoiding Type 2 undershoot.

4. CONCLUSION

In this article, we clarified the initial conditions for avoiding Type 1 undershoot in the initial response and confirmed the response using two methods for circular path-following control of a two-wheeled vehicle. The first method is to apply the rotational coordinate transformation to the vehicle transformed into the time-state control form, and the other is to apply the expansionary coordinate transformation in addition to the rotational one. We clarified that the second method avoided Type 1 undershoot more easily than the first by deriving the conditions for avoiding the undershoot response. Further, we found that Type 2 undershoot occurred after the initial response, although Type 1 undershoot was avoided in some initial conditions. Therefore, we examined the conditions for Type 2 undershoot within the limited range of the initial conditions of the vehicle. We verified that Type 2 undershoot occurred in the first method, but not in the second. The conditions for Type 2 undershoot need to be minutely considered in future studies.

ACKNOWLEDGEMENTS

This work was supported by JSPS KAKENHI Grant Number JP21H01350.

REFERENCES

Rosas-Vilchis, A., de Loza, A. F., Aguilar, L. T., Cieslak, J., Henry, D., and Montiel-Ross, O. (2020). Trajectory tracking control for an AutoNOMO vehicle using a decoupling approach. 2020 28th Mediterranean Conference on Control and Automation (MED), pp. 375-380.

Iida, M., Uchida, R., Zhu, H., Suguri, M., Kurita, H., and Masuda, R. (2013). Path-following control of a head-feeding combine robot. Engineering in Agriculture, Environment and Food, 6(2), pp. 61-67.

Sutisna, S. P., Setiawan, R. P. A., Subrata, I. D. M., Mandang, T. (2021). Tracking control of an autonomous head feeding combine. Instrumentation Mesure Metrologie, vol. 20, no. 2, pp. 85-90.

Egami, T., Motizuki, K., and Nakazaki, S. (2005). A New Path Control for Vehicles to Desired Arbitrary Curve Paths. Transactions of the Society of Instrument and Control Engineers, vol. 41, no. 1, pp. 85-87(in Japanese).

Egami, T., and Tsuburaya, Y. (2004). A path control with vector decomposition by means of expansionary coordinate transformations. IEEJ Trans. on Industry Applications, vol. 123, no. 12, pp. 1474-1482(in Japanese).

Sampei, M. (1994). A control strategy for a class of non-holonomic systems-time state control form and its application. Proc. 33rd CDC, pp. 1120-1121.

Sampei, M., Kiyota, H., Koga, M., and Suzuki, M. (1996). Necessary and sufficient conditions for transformation of nonholonomic system into time-state control form. Proc. 35th CDC, pp. 4745-4746.

Nakata, R., Tanamura, M., Chida, Y., and Mitsuhashi, T. (2020). Undershoot in a circular path following the control response of a two-wheeled vehicle. Proc. Dynamics and Design Conference 2020, no. 20-11(in Japanese).

Norimatsu, T., and Ito, M. (1961). On the zero non-regular control system. IEEJ, vol. 81, no. 871, pp. 566-575(in Japanese).

Mita, T., and Yoshida, H. (1981). Undershooting phenomenon and its control in linear multivariable servomechanisms. IEEE Trans. on Automatic Control, vol. 26, no. 2, pp. 402-407.

Hara, S., and Kondo, R. (1986). Design of non-undershooting multivariable servo systems using dynamic compensators. International. Journal of Control, vol. 27, no. 3, pp. 361-386.

Deodhare, G., and Vidyasagar, M. (1992). Control system design via infinite linear programming. Int. J. Control, vol. 55, pp. 1351-1380.

De La Barra, B. L., El-Khoury, M., and Fernandez, M. (1996). On undershoot in scalar discrete-time systems. Automatica, vol. 32, no. 2, pp. 255-259.

Nakata, R., Tanamura, M., Chida, Y., and Mitsuhashi, T. (2021). Undershoot response analysis of circular path-following control of an autonomous vehicle. Mechanical Engineering Journal, vol. 8, no. 2, p. 21-00002.

Murray, R. M., and Sastry, S. S. (1993). Nonholonomic motion planning: steering using sinusoids. IEEE trans. on Automatic Control, vol. 38, no. 5, pp. 700-716.

Brockett, R. W. (1983). Asymptotic stability and feedback stabilization, differential geometric control theory. Progress in Mathematics, vol. 27, pp. 181-191.